

# Minimizing the linewidth of the Flux-Flow Oscillator

A.L. Pankratov\*

*Institute for Physics of Microstructures of RAS, Nizhny Novgorod, Russia*

For the first time the linewidth of Flux-Flow Oscillator has been calculated by direct computer simulation of the sine-Gordon equation with noise. Nearly perfect agreement of the numerical results with the formula derived in [Phys. Rev. B, **65**, 054504 (2002)] has been achieved. It has been demonstrated that for homogeneous bias current distribution the linewidth actually does not depend on the junction length for practically interesting parameters range. Depending on the length of the unbiased tail, the power may be maximized and the linewidth may be minimized in a broad range of bias currents. The linewidth can be decreased further by 1.5 times by proper load matching.

PACS numbers:

During the last decade the flux-flow oscillator (FFO), based on a viscous flow of magnetic flux quanta in a long Josephson tunnel junction (JTJ) [1], has been considered as the most promising local oscillator in superconducting spectrometers [2] for space-born radio astronomy and atmosphere monitoring due to its wide operational bandwidth and easy broadband tunability. However, the spectral linewidth of the emitted radiation of the free-running FFO is rather large, that complicates the phase locking. Typically, the free-running linewidth is 2-20 MHz for an Nb-AlO<sub>x</sub>-Nb FFO in the 400-700GHz frequency range. For spectral applications it is of crucial importance to reduce the FFO linewidth, to make it more homogeneous in all working frequency range, and to increase the emitted power to improve the signal-to-noise ratio.

The dynamical and fluctuational properties of the FFO have been investigated in [1]-[20], in particular, the linewidth has been studied both experimentally [7]-[13] and theoretically [14]-[18]. However, the only formula for the linewidth, derived in [17], that takes into account not only differential resistance over bias current, but also differential resistance over magnetic field, has been proven as the most adequately describing experimental results, see [10],[11]. But, the nature of conversion of bias current fluctuations to the magnetic field fluctuations is still unclear, and the conversion factor is not known exactly. Also, the dependence of the linewidth on the bias current profile and certain parameters, such as RC-load, has not been systematically studied yet neither theoretically nor experimentally. The aim of the present paper is to study the FFO linewidth by direct computer simulation of the sine-Gordon equation with noise, to compare the obtained results with the formula of [17] and to make certain optimizations of FFO design (varying bias current profile and the RC-load) in order to minimize the linewidth and to increase the emitted power.

For several decades the sine-Gordon model has been the most adequate model for the long Josephson junction, giving a good qualitative description of its basic properties:

$$\phi_{tt} + \alpha\phi_t - \phi_{xx} = \beta\phi_{xxt} + \eta(x) - \sin(\phi) + \eta_f(x, t), \quad (1)$$

where indices  $t$  and  $x$  denote temporal and spatial derivatives, respectively. Space and time are normalized to the Josephson penetration length  $\lambda_J$  and to the inverse plasma frequency  $\omega_p^{-1}$ , respectively,  $\alpha = \omega_p/\omega_c$  is the damping parameter, where  $\omega_p = \sqrt{2eI_c/\hbar C}$ ,  $\omega_c = 2eI_c R_N/\hbar$ ,  $I_c$  is the critical current,  $C$  is the JTJ capacitance, and  $R_N$  is the normal state resistance,  $\beta$  is the surface loss parameter,  $\eta(x)$  is the dc overlap bias current density, normalized to the critical current density  $J_c$ , and  $\eta_f(x, t)$  is the fluctuational current density. In the case where the fluctuations are treated as white Gaussian noise with zero mean, and the critical current density is fixed, its correlation function is:  $\langle i_f(x, t)i_f(x', t') \rangle = 2\alpha\gamma\delta(x-x')\delta(t-t')$ , where  $\gamma = I_T/(J_c\lambda_J)$  is the dimensionless noise intensity [20],  $I_T = 2ekT/\hbar$  is the thermal current,  $e$  is the electron charge,  $\hbar$  is the Planck constant,  $k$  is the Boltzmann constant and  $T$  is the temperature.

The boundary conditions, that simulate simple RC-loads, see Ref.s [3] and [19], have the form:

$$\phi(0, t)_x + r_L c_L \phi(0, t)_{xt} - c_L \phi(0, t)_{tt} + \quad (2)$$

$$\beta r_R c_R \phi(0, t)_{xtt} + \beta \phi(0, t)_{xt} = \Gamma - \Delta\Gamma,$$

$$\phi(L, t)_x + r_R c_R \phi(L, t)_{xt} + c_R \phi(L, t)_{tt} + \quad (3)$$

$$\beta r_R c_R \phi(L, t)_{xtt} + \beta \phi(L, t)_{xt} = \Gamma + \Delta\Gamma.$$

Here  $\Gamma$  is the normalized magnetic field,  $\Delta\Gamma = 0.05\Gamma$  is a small magnetic field difference, see [19], and  $L$  is the dimensionless length of JTJ. The dimensionless capacitances and resistances,  $c_{L,R}$  and  $r_{L,R}$ , are the FFO RC-load placed at the left (output) and at the right (input) ends, respectively. It should be noted that, following Ref. [18], if both overlap  $\eta_{ov} = (1/L) \int_0^L \eta(x)dx$  and inline  $\eta_{in} = 2\Delta\Gamma/L$  components of the current are present, the total current,  $\eta_t$ , with respect to which all current-voltage characteristics will be computed, is the sum of overlap and inline components:  $\eta_t = \eta_{ov} + \eta_{in}$ .

In Ref. [19] on the basis of Eq. (1) without noise and boundary conditions (2), (3), the investigation of current-voltage characteristics of FFO has been performed. For the bias current profile, depicted in the inset of Fig. 1 by curve with crosses, good qualitative agreement with experimental IVCs has been achieved. Due to experimental

motivation it was assumed, that the current profile was parabolic (with the curvature  $a = 0.005$ ) between the left and the right boundaries of bias electrode  $x_0$  and  $x_1$  ( $0 \leq x_0 \leq x_1 \leq L$ ), and drops down exponentially in the unbiased tails  $x \leq x_0$ ,  $x \geq x_1$  with the decay factor  $p$ :  $\exp(-px)$  (with  $p = 0.13$  in Fig. 1). The decay factor and the parabolic curvature were used as fitting parameters when the comparison with the experimental IVCs was done.

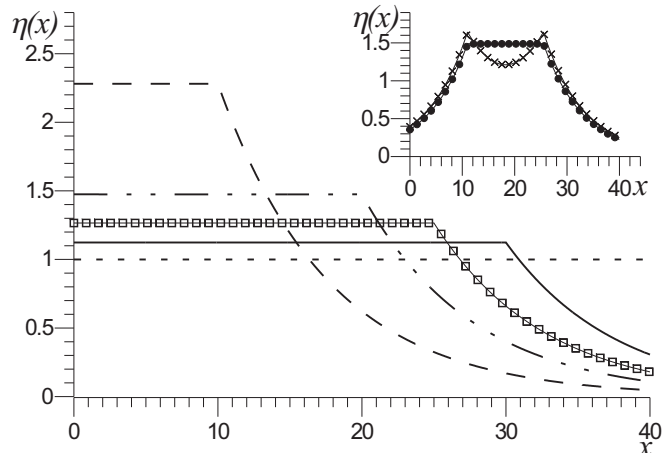


FIG. 1: The distribution of overlap component of bias current  $\eta(x)$ . Short-dashed line - homogeneous distribution; solid curve -  $x_1 = 30$ ; curve with rectangles -  $x_1 = 25$ ; dot-dashed curve -  $x_1 = 20$ ; long-dashed curve -  $x_1 = 10$ . Inset: curve with circles -  $x_0 = 11$ ,  $x_1 = 25.5$ ,  $a = 0$ ; curve with crosses -  $x_0 = 11$ ,  $x_1 = 25.5$ ,  $a = 0.005$ .

The key question arises: if one will change the lengths of unbiased tails, how it will affect the emitted power and the linewidth? In Ref. [1] it was suggested to use the unbiased tail to decrease the differential resistance  $r_d$  that might reduce the linewidth, if the formula for the linewidth of short JTJ would work for FFO (here and below the linewidth is defined as full width, half power):

$$\Delta f_s = 2\alpha\gamma r_d^2/L. \quad (4)$$

Later, it was found experimentally [9], that even for small  $r_d$  the FFO linewidth is almost one order of magnitude larger than predicted by (4). In Ref. [17], the formula for the FFO linewidth, that takes into account not only conventional differential resistance over bias current, but also differential resistance over magnetic field  $r_d^{CL} = Ldv/d\Gamma$  (control line current) was derived:

$$\Delta f_{FFO} = 2\alpha\gamma(r_d + \sigma r_d^{CL})^2/L, \quad (5)$$

and demonstrated good agreement with experiment [10],[11]. In Ref. [6] it has been demonstrated that by the choice of the bias current profile, the radiation can be either enhanced or suppressed, and it is desirable to supply more bias current at the radiating end, than at

the input end. Therefore, in the frame of the present paper we shift the current profile to the left,  $x_0 = 0$ , and vary the length of unbiased tail, which is located at the right end of JTJ. Also, to avoid problems with scaling of parabolic curvature (it is not clear what to keep constant, the curvature or the depth of the "well"), let us set the current profile to be constant between  $x_0$  and  $x_1$ .

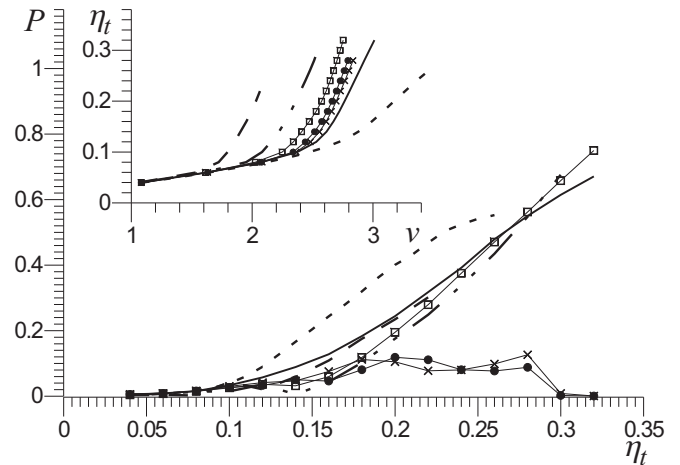


FIG. 2: Radiated power versus total current, computed for  $\eta(x)$ , presented in Fig. 1: short-dashed line - homogeneous distribution; solid curve -  $x_1 = 30$ ; curve with rectangles -  $x_1 = 25$ ; dot-dashed curve -  $x_1 = 20$ ; long-dashed curve -  $x_1 = 10$ ; curve with circles -  $x_0 = 11$ ,  $x_1 = 25.5$ ,  $a = 0$ ; curve with crosses -  $x_0 = 11$ ,  $x_1 = 25.5$ ,  $a = 0.005$ . Inset: dc current-voltage characteristics computed for  $\eta(x)$ , presented in Fig. 1: the notations are the same as for power.

The power at RC-load at the radiating end  $x = 0$  for different bias current profiles depicted in Fig. 1, is presented in Fig.2. The power is computed in accordance with [3]. The implicit difference scheme, used to solve Eq. (1) with noise, has been successfully tested in [20] when the mean escape times from zero voltage state were investigated. The parameters are the following:  $L = 40$ ,  $\alpha = 0.033$ ,  $\beta = 0.035$ ,  $c_L = c_R = 100$ ,  $r_L = 2$ ,  $r_R = 100$ ,  $\Gamma = 3.6$ , and  $\gamma = 0.1$ . From Fig. 2 one can see, that for the case of two unbiased tails  $x_0 = 11$ ,  $x_1 = 25.5$  the power is minimal and almost order of magnitude smaller than for the current profile with the one unbiased tail  $x_1 = 25$ , which gives maximal power among all considered current profiles. In the inset of Fig. 2 the current-voltage characteristics for the same current profiles are given for comparison: it is seen, that the flux-flow steps have largest height also for  $x_1 = 25$ . The height of IVCs for both profiles with  $x_0 = 11$ ,  $x_1 = 25.5$  and  $a = 0.005$ ,  $a = 0$  have close values to each other and are comparable to  $x_1 = 25$ . So, it is desirable to give larger bias current at the radiating end to get larger emitted power. It should be noted that for both profiles with two unbiased tails, the power versus bias current has minima as in experiment [13]. However, the investigation of this phenomenon is out of scope of the present paper and will

be presented elsewhere.

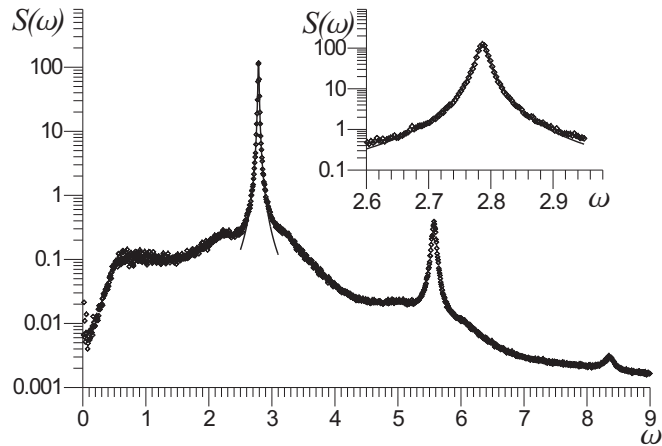


FIG. 3: The calculated spectral density for  $x_1 = 25$ ,  $\eta_0 = 0.3$ ,  $\gamma = 0.1$  - diamonds; Lorentzian approximation - solid curve. Inset: the same, enlarged around the spike.

The power spectral density of FFO was computed as Fourier transform of the correlation function of the second kind  $\Phi[\tau] = \frac{1}{T_{av}} \int_0^{T_{av}} \langle v_0(t)v_0(t+\tau) \rangle dt$ , where  $v_0(t) = d\varphi(t,0)/dt$  is the voltage at the RC-load ( $x=0$ ) and  $T_{av}$  is the averaging time. There are two general restrictions, that complicates the calculation of the spectral density and the linewidth: on one hand, the time step should be small enough to resolve oscillations, and the averaging time  $T_{av}$  should be rather large to resolve fine spectral spikes. Due to these restrictions the noise intensity was chosen  $\gamma = 0.1$ . Nevertheless, this is the same limit of low noise intensity as in experiments, since IVCs are almost unaffected by noise, the spectral spikes are narrow, and the linewidth perfectly scales proportionally to the noise intensity, see below. For the linewidth calculations the following parameters were used: spatial step  $\Delta x = 0.05$ , temporal step  $\Delta t \approx 0.1$ ,  $T_{av} = 8000$ .

In Fig. 3 the power spectral density of FFO is presented. As one can see, the emitted signal is nearly sinusoidal, in agreement with [3] and experimental results: the power contained in the second and third harmonics is much lower than in the main one. Also, the spectral peak is perfectly Lorentzian in more than two orders of magnitude interval.

In Fig. 4 the FFO linewidth versus differential resistance  $r_d$  for junctions of  $L = 40$  and  $\gamma = 0.1$  is presented for the case of homogeneous bias current distribution and  $x_1 = 30$ . It is seen, that in both cases formula (5) is in good agreement with numerical results, while formula (4) and formula from [16] (in formula (4)  $\alpha$  must be substituted by inverse static resistance  $\eta_t/v$ ) significantly underestimate the linewidth.

The appearance of the conversion of bias current fluctuations to magnetic field fluctuations may be explained in the following way: boundary conditions (2), (3) of Eq. (1) depend on the phase, which fluctuates, since it

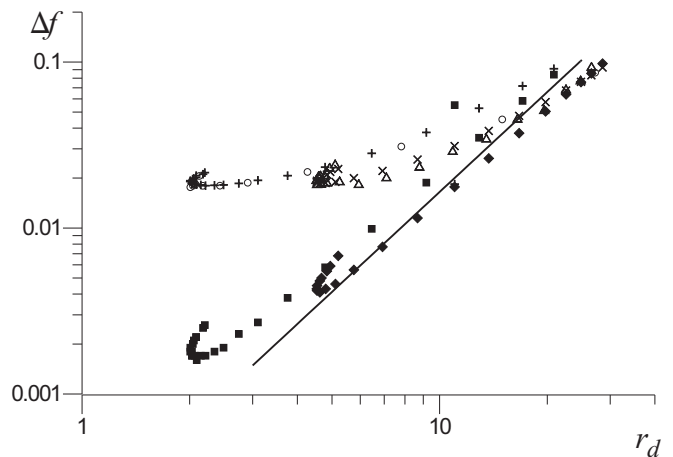


FIG. 4: FFO linewidth versus differential resistance  $r_d$  for  $L = 40$  and  $\gamma = 0.1$ . Empty triangles and crosses - simulations and theory (5) for homogeneous bias current distribution, empty circles and crosses - simulations and theory for the case with unbiased tail  $x_1 = 30$ , filled diamonds and rectangles - theory of [16], solid line - theory (4).

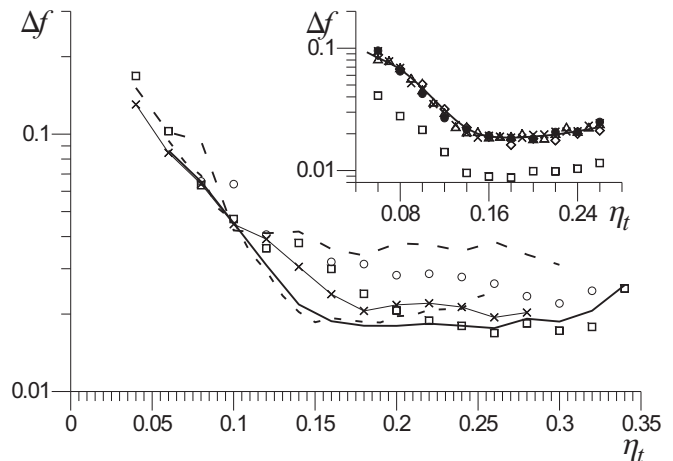


FIG. 5: FFO linewidth versus total current, computed for  $\eta(x)$ , presented in Fig. 1,  $\gamma = 0.1$ : short-dashed curve - homogeneous distribution; solid curve -  $x_1 = 30$ ; rectangles -  $x_1 = 25$ ; circles -  $x_1 = 20$ ; long-dashed curve -  $x_1 = 10$ ; curve with crosses -  $x_0 = 11$ ,  $x_1 = 25.5$ ,  $a = 0.005$ . Inset: FFO linewidth for junctions with different lengths:  $L = 20$  - diamonds,  $L = 40$  - crosses,  $L = 60$  - circles,  $L = 80$  - triangles, solid curve - theory for  $L = 60$ , all these curves for  $\gamma = 0.1$ ; rectangles - simulations for  $L = 40$ ,  $\gamma = 0.05$ .

is governed by Eq. (1) with noise. It is quite difficult to calculate the noise conversion factor  $\sigma$ , since it should be done self-consistently. In the following, to see how the linewidth behaves in all working range, let us plot it versus total bias current  $\eta_t$ .

Let us analyze the dependence of the linewidth on the length of unbiased tail. From Fig. 5 it is seen, that minimal value of  $\Delta f$  is reached for several cases, including the homogeneous one. However, for the unbiased tail

$x_1 = 30$ , the linewidth is nearly constant (and minimal) in a maximal range of bias currents. Therefore, the unbiased tail of 1/4 of junction's length gives the nearly maximal power and nearly minimal linewidth in broadest range of bias current, and can be recommended for spectral applications.

Let us investigate the dependence of the linewidth versus junction's length  $L$  for homogeneous bias current distribution. The corresponding curves are presented in the inset of Fig. 5. It is seen, that increase of  $L$  does not help to decrease the linewidth, the curves nearly coincide. The lowest curve is computed for noise intensity  $\gamma = 0.05$  and the linewidth is two times smaller than for  $\gamma = 0.1$ . Therefore, the noise intensity  $\gamma = 0.1$  is indeed rather low, and in the following one can get good estimate for experimental parameters by multiplication of the computed curve on the numerical factor  $\gamma_e/\gamma$ , where  $\gamma_e$  is the noise intensity, corresponding to the experiment.

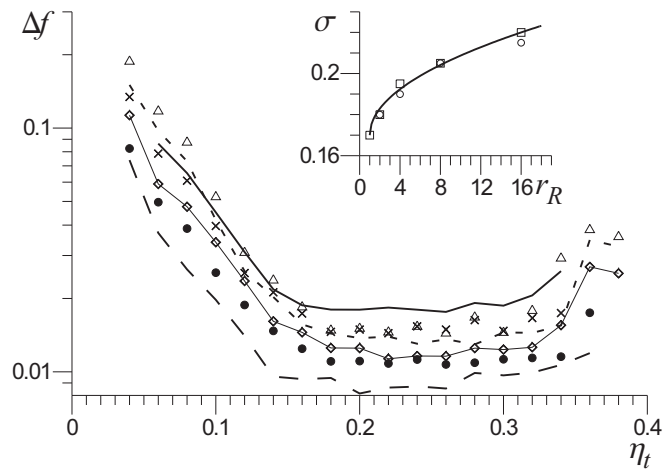


FIG. 6: FFO linewidth versus total current computed for different values of load resistances and noise intensity,  $x_1 = 30$ : solid curve -  $r_L = 2, r_R = 100$ ; triangles -  $r_L = r_R = 8$ ; crosses -  $r_L = 2, r_R = 8$ ; short-dashed curve -  $r_L = r_R = 4$ ; curve with diamonds -  $r_L = r_R = 2$ ; circles -  $r_L = r_R = 1$ ; all these curves for  $\gamma = 0.1$ ; long-dashed curve -  $r_L = 2, r_R = 100$  for  $\gamma = 0.05$ . Inset: the coefficient  $\sigma$  versus  $r_R$ , rectangles -  $r_L = r_R$ ; circles -  $r_L = 2$ ; solid curve - fitting by  $\sqrt{r_R}$ .

Normally, FFO radiating end  $x = 0$  is well matched to the external environment, while the opposite end is strongly mismatched, as it was modeled in [19] and in the present paper. It is interesting to analyze, how the linewidth will change, if the FFO is better matched at both ends. The results of this analysis are presented in Fig. 6 for  $x_1 = 30$ . It is seen, that improved matching at the opposite end can decrease the linewidth by 1.5 times. It is important to note, that equal matching at both ends gives smaller linewidth than perfect matching at the radiating end and bad at the opposite one, e.g., compare the curves for  $r_L = 2, r_R = 100$  and  $r_L = r_R = 4$  and note, that the curves for  $r_L = r_R = 8$  and

$r_L = 2, r_R = 8$  nearly coincide. Finally, it is important to mention, that the noise conversion factor  $\sigma$  perfectly scales as  $\sqrt{r_R}$  both for  $r_L = 2$ , and for  $r_L = r_R$ .

The linewidth of Flux-Flow Oscillator has been calculated by direct computer simulation of the modified sine-Gordon equation with noise which takes into account surface losses and RC load. Nearly perfect agreement of the computer simulation results with the formula (5) has been achieved. It has been demonstrated that for homogeneous bias current distribution the linewidth actually does not depend on the junction length for practically interesting parameters range. Depending on the length of the unbiased tail, the power may be maximized and the linewidth may be minimized in a broad range of bias currents. The linewidth can be decreased further by 1.5 times by proper load matching.

The work was supported by the ISTC project 3174.

\* Electronic address: alp@ipm.sci-nnov.ru

- [1] T. Nagatsuma, K. Enpuku, F. Irie, and K. Yoshida, J. Appl. Phys. **54**, 3302 (1983), see also **56**, 3284 (1984); **58**, 441 (1985); **63**, 1130 (1988).
- [2] V.P. Koshelets and S.V. Shitov, Supercond. Sci. Technol. **13**, R53 (2000).
- [3] C. Soriano, G. Costabile, and R.D. Parmentier, Supercond. Sci. Technol. **9**, 578 (1996).
- [4] M. Cirillo, et. al., Phys. Rev. B **58**, 12377 (1998).
- [5] M. Salerno and M.R. Samuelsen, Phys. Rev. B **59**, 14653 (1999).
- [6] A.L. Pankratov, Phys. Rev. B **66**, 134526 (2002).
- [7] V.P. Koshelets, A. Shchukin, I.L. Lapytskaya, and J. Mygind, Phys. Rev. B **51**, 6536 (1995).
- [8] A.V. Ustinov, H. Kohlstedt, and P. Henne, Phys. Rev. Lett. **77**, 3617 (1996).
- [9] V.P. Koshelets, S.V. Shitov, A.V. Shchukin, L.V. Filippenko, J. Mygind, and A.V. Ustinov, Phys. Rev. B **56**, 5572 (1997).
- [10] V. P. Koshelets, et. al., Supercond. Sci. Technol. **14** 1040 (2001).
- [11] V.P. Koshelets, et. al., Physica C **372-376**, 316 (2002).
- [12] V.P. Koshelets, et. al., Supercond. Sci. Technol. **17**, S127 (2004).
- [13] V.P. Koshelets, et. al., IEEE Trans. Appl. Supercond. **15**, 964 (2005).
- [14] A.A. Golubov, B.A. Malomed, and A.V. Ustinov, Phys. Rev. B **54**, 3047 (1996).
- [15] A.P. Betenev and V.V. Kurin, Phys. Rev. B **56**, 7855 (1997).
- [16] M. Salerno, M. Samuelsen, and A. Yulin, Phys. Rev. Lett. **86**, 5397, (2001).
- [17] A.L. Pankratov, Phys. Rev. B **65**, 054504 (2002).
- [18] J. Mygind, V.P. Koshelets, M. Samuelsen and A.S. Sobolev, IEEE Trans. Appl. Supercond. **15**, 968 (2005).
- [19] A.L. Pankratov, A.S. Sobolev, V.P. Koshelets, and J. Mygind, Phys. Rev. B **75**, 184516 (2007).
- [20] K.G. Fedorov and A.L. Pankratov, Phys. Rev. B **76**, (2007), in press.